

Electron correlation in a hard spherical external potential: Wigner molecule formation and hybridization

David C. Thompson and Ali Alavi*

Chemistry Department, University of Cambridge, Lensfield Road, Cambridge CB2 1EW, United Kingdom

(Received 7 October 2003; revised manuscript received 17 December 2003; published 12 May 2004)

We study a model of N electrons confined to a hard spherical box of radius R , for $N=3, 4$, and 5 . Unrestricted Hartree–Fock and full configuration-interaction calculations have been performed for high, medium, and low density regimes. Remarkable changes in electronic structure can be induced by varying the effective Coulomb coupling. A low-spin→high-spin transition occurs in the case of $N=4$ as R is increased. We demonstrate a close connection between the propensity to form hybrid orbitals and the onset of Wigner molecule formation.

DOI: 10.1103/PhysRevB.69.201302

PACS number(s): 73.21.–b, 31.10.+z, 73.22.–f

Studying electron correlation in model systems is a powerful way to obtain insight into complex phenomena associated with it. In atomic and molecular systems, a distinction is often made between dynamical and non-dynamical correlation, the former being the principal type of correlation in the light atoms, implying that the electrons move so as to avoid each other in the short range. On the other hand, non-dynamical correlation is responsible for localizing electrons on separated atomic sites, as in molecular dissociation, and is cause for considerable difficulties in molecular-orbital type theories (e.g., Hartree–Fock and Kohn–Sham). Such correlation arises ultimately through a superposition of uncorrelated determinants of the same symmetry.

In this paper we study the evolution of few-electron wave functions in a purely spherical geometry which exhibits several aspects of electron correlation. Our model consists of a spherical box of radius R , which contains a fixed number, N , of electrons, and is a generalization of recent work on the corresponding two-electron system.^{1–3} The box acts as a hard wall to confine the electrons. This system can be viewed as an idealization of a three-dimensional quantum dot, or “artificial atom.” By increasing R , we proportionately increase the effective Coulomb coupling between the electrons. The large R limit gives rise to Wigner molecule formation (finite versions of Wigner crystallization). In this state, the electrons (quasi-) localize in such a way as to minimize their mutual Coulomb repulsion. The correlation in this limit is non-dynamical. We observe that the shape of the emergent Wigner molecules bears a striking resemblance to the hybrid orbitals of conventional chemistry. Thus the three-electron system may be imagined to evolve from an s^2p configuration to an sp^2 configuration, the latter corresponding to an equilateral triangle, precisely the shape required to minimize the Coulomb repulsion between the three electrons. Similarly, for the four-electron system, an $s^2p^2 \rightarrow sp^3$ transition minimizes the Coulomb repulsion of the electrons through the formation of a *tetrahedral* Wigner molecule. Thus the physics of electron–electron repulsion already contains the seeds required to form hybrid states. This presents a radically different mechanism for what drives the formation of hybrid states than that provided by the classical theory of hybridization of Pauling.^{4,5} The latter is based upon a degenerate perturbation theory argument in which the external perturbation of the bonding atoms plays the decisive role in generating

directed bonds. We show, instead, that the onset of Wigner molecule formation at low electron densities (or in effect the Wigner–Seitz radius $r_s = R/N^{1/3}$) greatly enhances the propensity to form hybrid states.

The Hamiltonian for the problem can be written as (in atomic units):

$$\hat{H} = -\frac{1}{2} \sum_i^N \nabla_i^2 + \sum_i v_{\text{ext}}(\mathbf{r}_i) + \sum_{i < j} \frac{1}{|\mathbf{r}_i - \mathbf{r}_j|}, \quad (1)$$

$$v_{\text{ext}}(\mathbf{r}) = \begin{cases} 0, & r < R \\ \infty, & r > R. \end{cases} \quad (2)$$

We performed unrestricted Hartree–Fock (UHF) and full configuration-interaction (FCI) for the ground state of this Hamiltonian as a function of R . The model presents an interesting opportunity to see how UHF theory performs for various R , since both dynamical and non-dynamical correlation are present. The appropriateness of UHF theory to describe Wigner crystallization/molecule formation is itself a topical issue.^{6–8} FCI provides an essentially exact description of the ground state including the correct spin S , but requires a great number of determinants whose interplay produces the desired correlation. The physical interpretation of the FCI solution is not straightforward. In addition achieving convergence severely limits the number of electrons which can be studied. In this paper we report results up to $N=5$. These provide benchmarks with which we can judge both the quantitative and qualitative accuracy of the UHF theory.

A suitable one-electron basis set in which both the UHF and the FCI calculations can be performed consists of a product of a spherical Bessel function j_l and a spherical harmonic Y_{lm} :

$$u_{nlms}(\mathbf{r}, \sigma) = j_l(\alpha_{nl}r) Y_{lm}(\theta, \phi) \delta_{\sigma s}. \quad (3)$$

The α_{nl} are chosen so that the orbitals vanish at the sphere boundary. At variance with hydrogenic orbitals, the l quantum number is not restricted to be $< n$. The energetic ordering of the levels is well known:⁹ $1s < 1p < 1d < 2s < 1f < 2p \dots$. If we neglect electron–electron interaction we obtain the following periodic table of artificial elements based on the *aufbau* principle for $N=2-8$: $1s^2$ (helium-like), $1s^2 1p$ (boron-like), $1s^2 1p^2$ (carbon-like), $1s^2 1p^3$ (nitrogen-like), $1s^2 1p^4$ (oxygen-like), $1s^2 1p^5$ (fluorine-

TABLE I. Summary of energies from HF and FCI computed in this study, at $R=1,5,20$. The transition density r_s^* is also given where appropriate. The basis sets used for the $N=3-5$ FCI calculations are, respectively: $1g2g3g4f$, $1g2f3d4s$, $1f2d3p4p$, corresponding to 998 260, 4 249 575, 8 936 928 determinants.

N	E_{RHF}	E_{UHF}		E_{FCI}	
		$m_s = \frac{1}{2}$	$\frac{3}{2}$	2P	4P
3					
$R=1$		24.5776	28.9578	24.5026	28.9402
$R=5$		1.6852	1.7498	1.6292	1.7354
$R=20$		0.2350	0.2350	0.2251	0.2275
r_s^*		7.12			
4		$m_s=1$	2	3P	5S
$R=1$	39.0553	38.8311	42.9533	38.7287	42.9168
$R=5$	2.9315	2.8815	2.9046	2.8038	2.8752
$R=20$	0.4748	0.4337	0.4329	0.4184	0.4175
r_s^*		3.81		8.69	
5		$m_s = \frac{3}{2}$	$\frac{5}{2}$	4S	6D
$R=1$	54.3943	64.6182	54.2663	64.5785	
$R=5$	4.3277	4.5386	4.2273	4.5080	
$R=20$	0.6977	0.6970	0.6726	0.6841	
r_s^*		9.84			

like), and $1s^21p^6$ (neon-like). The effect of increasing the sphere radius R is to scale the energetic spacing between the levels by $1/R^2$, and thereby allowing for an increase in the amount of electron correlation present.

The (Pople–Nesbet) UHF equations were solved in a basis with $n_{\text{max}}=l_{\text{max}}=3$, sufficient to give converged results for the systems $N=3-5$ studied.¹⁰ Some UHF energies are

reported in Table I. Where relevant, we have computed all possible multiplicities, but to keep the table manageable, we give only the two competitive ones. We give $R=1,5,20$ as representative of high, medium, and low densities. We have also, for reference, provided the *restricted* Hartree–Fock energies as well. The results show that the fully spin-polarized state is always (marginally) more stable than the lower m_s states for sufficiently large R . The transition density (r_s^*) depends sensitively on N .¹¹ In particular, at $N=4$, this occurs at the relatively high density of $r_s^* \approx 3.8$, whereas at $N=3$ and 5, it occurs at the rather lower densities of $r_s^* \approx 7.1$ and 9.8, respectively. By examining the kinetic, Coulomb, and exchange contributions to the total energy of the UHF wave function, we found that the stabilization of the high-spin state in the large R limit is due to both lower Coulomb energies *and* more favorable exchange energies.

To obtain insight into the character of the UHF wave functions, we performed a population analysis using the UHF density matrix $P_{\mu\nu}$, where $\mu=\{nlms\}$ is an index identifying a one-electron basis function. Let $p_l = \sum_{\mu\mu\in l} P_{\mu\mu}$; p_l gives the total population of the l th angular momentum component in the wave function, providing a convenient measure of the number of s, p, d, \dots electrons. Shown in Fig. 1 are plots of p_l as a function of R . Considering $N=3$, $m_s = \frac{1}{2}$, for $R < 2.5$, the s -population is very close to 2, while the p -population is close to 1 (with a negligible amount of d); as expected the character of the wave function is s^2p . In this limit, the system is effectively monovalent, i.e., we would expect an external perturbing potential to couple only to the p -electron. As R is increased, between 2.5 and 5 a.u., we obtain a slow decrease in the s -population, with a concomitant rise in d -character, followed by a precipitous increase in p character when $R \approx 5$, accelerating the

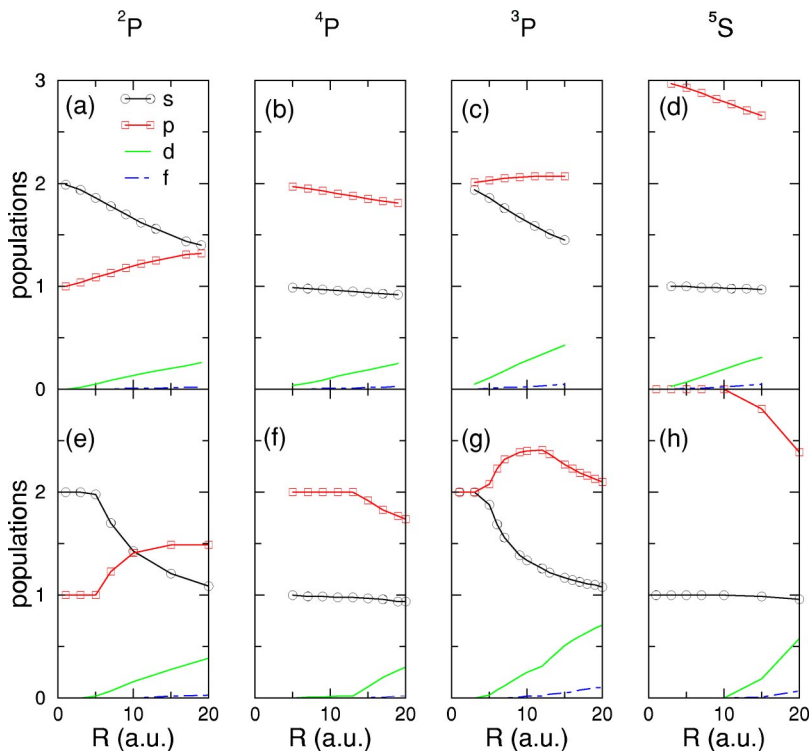


FIG. 1. (Color online) Angular-momentum decomposed population analyses. The upper panel refer to FCI wave functions; the lower panel to UHF. (a) $N=3$ 2P ; (b) $N=3$ 4P ; (c) $N=4$ 3P ; (d) $N=4$ 5S ; (e) $N=3$ $m_s=1/2$; (f) $N=3$ $m_s=3/2$; (g) $N=4$ $m_s=1$; (h) $N=4$ $m_s=2$.

TABLE II. Breakdown of the kinetic and potential energies of the FCI wave functions for the three-, four-, and five-electron systems in the large sphere limit ($R=20$).

N	$\langle T \rangle$	$\langle U \rangle$	$\langle E \rangle$
3 (2P)	0.0751	0.1500	0.2251
(4P)	0.0794	0.1481	0.2275
4 (3P)	0.1199	0.2986	0.4184
(5S)	0.1210	0.2965	0.4175
5 (4S)	0.1624	0.5102	0.6726
(6D)	0.1740	0.5101	0.6841

drop in s -character. However, even in the large R limit, the p -population appears to plateau at approximately 1.5. A non-negligible amount of d -character arises. A similar population analysis for the $m_s = \frac{3}{2}$ (fully spin-polarized) state shows the character of this state to be very nearly sp^2 for all R studied, with a slow, gradual decline in s - and p -character in the large R limit, with a concomitant rise in the d -character. In this latter situation, we expect all three electrons to be able to couple effectively to an external perturbation, making the system sp^2 tri-valent.

Turning now to the FCI calculations, these provide us with wave functions which are eigenstates of the \hat{L}^2 and \hat{S}^2 operators, and can therefore be assigned term symbols. We first examined the rate of convergence of the energies of different states with respect to basis set size. Of importance is to establish energies which are sufficiently well converged to distinguish between different S states. This turned out to be a delicate matter at large R , particularly for $N=3$, for which the two competing states (2P and 4P) are close in energy.¹² For the largest basis sets, we obtain a convergence of a few parts in 10^5 , sufficient to discriminate between the two states which differ in 1 part in 10^3 (Table I). Unlike the UHF theory, the low-spin state is the true ground state for the $N=3$ system, even in the Wigner crystal limit. It is interesting to ask why the 2P state is lower in energy than the 4P . To this end, we show the breakdown of the total energy E into its kinetic and Coulomb components in Table II. This shows that, in the Wigner molecule limit, the high-spin state has, indeed, a lower Coulomb energy than the corresponding low-spin ground-state. However, its kinetic energy is sufficiently higher to off-set this gain. The pair-correlation function $\rho_2(\mathbf{r}, \mathbf{r}')$ for 2P and 4P (Fig. 2) show how the correlations in these two states evolve with increasing R , and how they differ. The 2P has a liquid-like correlation at high density, exhibiting a single peak, diametrically opposite the reference particle. With increasing R , this peak eventually splits into two broad peaks, revealing a Wigner-molecule correlation. The 4P state has a two-peaked pair-correlation even at high densities, which increasingly localize in the large R limit. This explains the lower Coulomb energy associated with the 4P state.

In order to compare the qualitative nature of the FCI wave functions with that of the UHF theory, we computed the natural orbitals¹⁴ from the FCI first-order density matrix, and submitted them to a population analysis. The results are

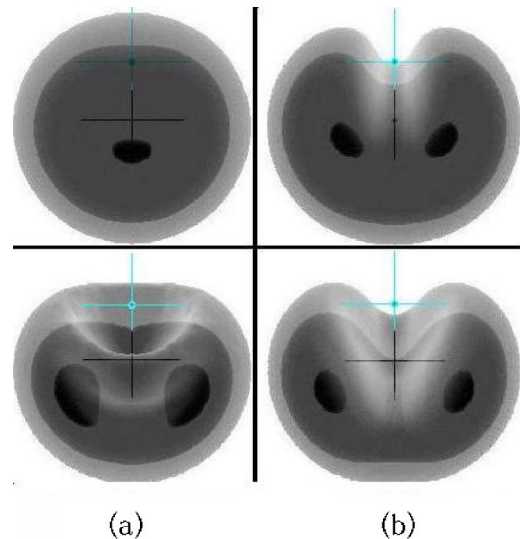


FIG. 2. Surface plots of the pair-correlation function for the three-electron system. (a) 2P , ($M_L=1$), (b) 4P , ($M_L=0$) states. The top panel: $R=1$, lower panel $R=20$. The reference electron (marked by the dot) has been placed at $R/2$ along the x axis, and the pair correlation function is displayed in the xy plane. The “seed”-like structures represent surfaces of greatest density.

shown in Figs. 1(c) and 1(d). We see that the 2P state, i.e., the ground state, has largely s^2p character, but with an increasing number s -holes which is apparent even at the high density of $R=2.5$ ($r_s=1.7$). This reflects the configuration interaction present in the FCI wave function. The number of s -holes increases smoothly, with a more gradual rise in the number of p - and d -electrons. The 4P state, which is marginally higher in energy, has largely sp^2 character, with an increase in s - and p -holes with increasing R .

For $N=4$, more complex behavior is seen in the UHF wavefunction [Figs. 1(g) and 1(h)]. For the $m_s=1$ state, at high density, the population analysis gives s^2p^2 character. In this limit, the system is divalent. With increasing R , at about $R=3.2$, the number of s -electrons begins to fall toward 1, and the number of p -electrons starts to rise toward a value between 2 and 3. However, for sufficiently large R , the amount of p -character begins to fall toward 2. A noticeable amount of d -character appears. In the large R limit, the $m_s=1$ wave function can be characterized as being sp^2d . On the other hand, the fully spin polarized ($m_s=2$) wave function has nearly perfect sp^3 character. This provides an explanation for the readiness by which the high-spin state UHF wave function is stabilized: it is capable of forming a tetrahedral hybrid state which lowers the Coulomb repulsion more effectively than the sp^2d configuration of the low-spin Wigner molecule.

The FCI calculations for the $N=4$ system exhibit behavior rather in line with the UHF results. The ground-state wave function is 3P at high density and 5S at low density, the transition between the two occurring at $R=13.79$, ($r_s=8.69$). A striking similarity exists with the spectrum of the carbon atom, which possesses a low-lying 5S state with $2s2p^3$ character.¹³ Table II shows that at low density the Coulomb energy of the 5S state is lower than that of 3P ,

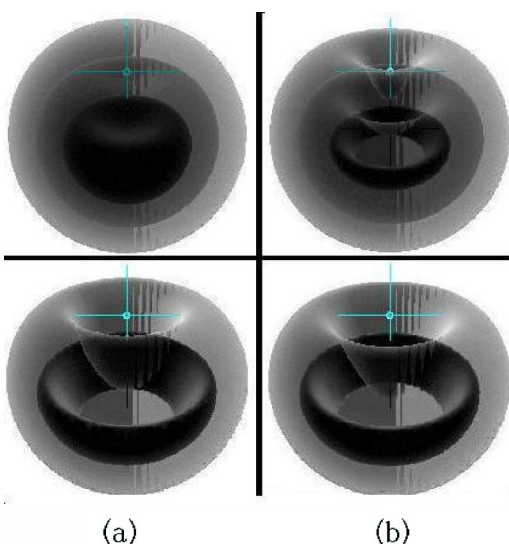


FIG. 3. Pair-correlation functions for the $N=4$ system. (a) ${}^3P, M_L=1$, (b) 5S states. The reference particle is placed at $R/2$ along the z axis. Azimuthal symmetry is maintained throughout, giving rise to the formation of a “ring” structure in the pair-correlation function. In the 3P state, the depletion of probability in the region of space diametrically opposite the reference particle is the signature of a Wigner molecule.

while the kinetic energy, though higher, does not offset this gain. Overall the total energy in the two states is a delicate balance. Examining the pair-correlation functions (Fig. 3) provides a visual indication of the changing electron correlation in the two states. Similar to the $N=3$ system, the 3P exhibits a liquid-like peak at high density. As R increases, this peak is smeared into a ring (maintaining azimuthal sym-

metry with respect to the reference particle), as one would expect of a tetrahedral molecule. However, the 5S state has this characteristic ring structure of a Wigner molecule even at high density.

In the 3P state, it is noticeable that with increasing R , the p population does not grow rapidly beyond 2, whereas the s population drops from 2 toward 1, with d -population rising toward 1. Thus the 3P large sphere limit has sp^2d character, very similar to that obtained by the low-spin UHF wave function. Thus the low-spin UHF wave function maintains a quite remarkable faithfulness in its character with respect to the 3P wave function in a regime we would expect it to do rather poorly.

With increasing number of electrons, a pattern begins to emerge. For the five-electron system (N -like), both UHF and FCI calculations point to a trivalent \rightarrow pentavalent (trigonal-bipyramid) cross-over to occur in the large sphere limit, mirroring the change in valence between N and P . Similarly, for the six-electron system (oxygen-like), increasing R changes the character from divalent to hexavalent (octahedral). The latter mimics the difference in valence that is observed between oxygen (divalent) and sulphur (hexavalent).

In summary, we have presented UHF and FCI calculations on a model few-electron system in a confined spherical potential. We show that the character of a many-electron wave function in such a geometry can acquire “hybrid” orbital characteristics at medium and low densities, purely as a consequence of electron–electron repulsion. There is a close connection with the formation of Wigner molecules. The UHF theory provides a reasonable description of the physics of this process, although its performance is much better for the four-electron problem than the three-electron problem.

*Electronic address: asa10@cam.ac.uk

¹A. Alavi, J. Chem. Phys. **113**, 7735 (2000).

²D.C. Thompson and A. Alavi, Phys. Rev. B **66**, 235118 (2002).

³J. Jung and J.E. Alvarillos, J. Chem. Phys. **118**, 10 825 (2003).

⁴L. Pauling, J. Am. Chem. Soc. **53**, 1367 (1931).

⁵See, e.g., R. McWeeny, *Coulson's Valence*, 3rd ed. (Oxford University Press, New York, 1979).

⁶For a review of this question, see, e.g., S.M. Reimann and M. Manninen, Rev. Mod. Phys. **74**, 1283 (2002).

⁷C. Yannouleas and U. Landman, Phys. Rev. Lett. **82**, 5325 (1999).

⁸J.R. Trail, M.D. Towler, and R.J. Needs, Phys. Rev. B **68**, 045107 (2003).

⁹L.D. Landau and E.M. Lifschitz, *Quantum Mechanics*, 3rd ed. (Pergamon, New York, 1985).

¹⁰The UHF wave functions were initiated by using a random orthonormalized set of vectors. In a few cases, solving the Pople–Nesbet equations in a large basis set from such an initial state proved difficult; we would converge into a stationary solution which was clearly not a minimum. In such cases, we used a (slightly randomized) minimal solution from a smaller basis set calculation as input for a larger basis set calculation. In all cases, we ensured the solutions were variational with respect to basis set, as they must be.

¹¹ r_s^* were computed using the false-position method to locate

where the difference in energy between the high spin and low spin configurations changed sign as a function of R . Typically four iterations were required to achieve an accuracy in r_s^* of 10^{-2} .

¹²Full details of convergence of the FCI calculations will be published in a forthcoming paper. Here we can give only a flavor of this. Let us indicate the basis set by giving l_{\max} for each n (e.g., $1d2p$ implies a basis set with $1s, 1p, 1d, 2s, 2p$ functions). For the minimal basis ($1p$) at $R=20$, we find the energy of the 2P state, $E({}^2P)=0.266\dots$, while $E({}^4P)=0.260\dots$. Increasing the basis to $1d2p$ we get $E({}^2P)=0.228\dots$, $E({}^4P)=0.231\dots$, reversing the order. Thereafter increasing the basis size lowers the energies without changing the order. Thus for the basis $1f2d3d4p$ we get $E({}^2P)=0.22513$, $E({}^4P)=0.22748$, and increasing further to $1g2g3g4f$ we obtain $E({}^2P)=0.22508$, $E({}^4P)=0.22748$, achieving a convergence of better than a few parts in 10^5 for both states.

¹³The ${}^3P-{}^5S$ splitting of carbon is 4.1826 eV (NIST Atomic Spectra database, www.nist.gov). If we fit R in our model to obtain this splitting, we obtain $R=3.89$. For smaller R , there are two other low-lying excited states, 1D and 1S , generated from the $1s^21p^2$ configuration. These conform with Hund's rules.

¹⁴See, e.g., R.G. Parr and W. Yang, *Density-Functional Theory of Atoms and Molecules* (Oxford University Press, New York, 1989).